

# PROCESS ANALYSIS OF MANUFACTURING THERMOPLASTIC TYPE-IV COMPOSITE PRESSURE VESSELS WITH HELICAL WINDING PATTERN

Martin Schäkel, Henning Janssen, Christian Brecher  
Fraunhofer Institute for Production Technology IPT  
Aachen, Germany

## ABSTRACT

Composite pressure vessels (CPVs) are widely employed for the high-pressure storage and transportation of hydrogen due to their extraordinary lightweight characteristics. Thermoset CPVs are the market standard due to easy and reliable production. The use of thermoplastic composites for CPV manufacturing via laser-assisted tape winding presents advantages with regard to out-of-autoclave and clean processing, recyclability and design freedom concerning the winding layup. The complex interactions of multiple process parameters like laser power, irradiation incidence angle and tape feed rate along the winding path influence the bonding quality within the composite laminate and require a thorough understanding, especially for helical winding patterns covering cylinder and dome parts of the pressure vessel. In this work, helical circuits of composite tape were placed on a thermoplastic liner with systematically varied process parameters. The temperature distribution governing the bonding quality between the tape plies was monitored and processed for data analysis. An empirical model characterizing the influences of process parameters on the nip point temperature was created highlighting differences in temperature variation on cylinder and dome parts. Tape feed rate profiles were also taken into account to identify action fields for the development of an optimized process for thermoplastic CPV manufacturing.

Corresponding author: Martin Schäkel

## 1. INTRODUCTION

In the course of shaping the future of mobility, the fuel-cell electric vehicles (FCEV) present a key technology for the automotive industry. Given the advantages of high driving ranges and easy, fast refueling, it is especially appealing for heavy vehicles like trucks, trains, buses and ambulances, which can be fueled at one or several stationary locations they frequently visit [1]. Among the technologies to be developed and challenges to overcome for a widespread development and adaption of fuel-cell vehicles, the storage of hydrogen is one of the most important [2]. Lightweight materials like fiber-reinforced plastics enable an efficient and safe storage of the gaseous hydrogen and therefore composite pressure vessels have gained a lot of market interest in recent years [3]. For these highly stressed components, carbon fiber-reinforced composites figure to be in high demand, given their high strength and stiffness properties combined with low weight and outstanding thermal and chemical properties [4]. Compared with metal parts, composites enable high fuel efficiency and lower emissions, satisfying newly arising regulations and requirements for the industry [3,4]. The main challenge lies within the development of economic composite manufacturing technologies for high-volume production, allowing for the integration of composite materials in automotive production lines [4].

*Copyright 2021. Used by the Society of the Advancement of Material and Process Engineering with permission.*

## 1.1 Composite pressure vessels

Based on the material composition, five types of composite pressure vessels (CPVs) are defined: While Type I characterizes an all-metal design, Types II and III combine a metal inner body, termed “liner”, which either a composite reinforcement of the cylindrical area (Type II) or the entire liner including cylinder and domes (Type III). The higher the mass fraction of composite reinforcement, the lower the weight and the higher the material costs of the component. The reduction of weight allows for higher fuel economy and load-carrying capacity. Other advantages of composite application in pressure vessels with respect to metals include increased gas containment pressures, increased energy storage density, better corrosion resistance and fatigue resistance leading to better safety. For those reasons, composite pressure vessels are the standard for hydrogen storage. Types IV and V designate all-composite designs, with Type IV applying the reinforcement around a plastic liner, while Type-V vessels are manufactured without liner [3]. Figure 1 shows a Type-IV 40-liter pressure vessel consisting of a thermoplastic liner, thermoplastic composite reinforcement and boss parts with metal threads for connection to external systems.

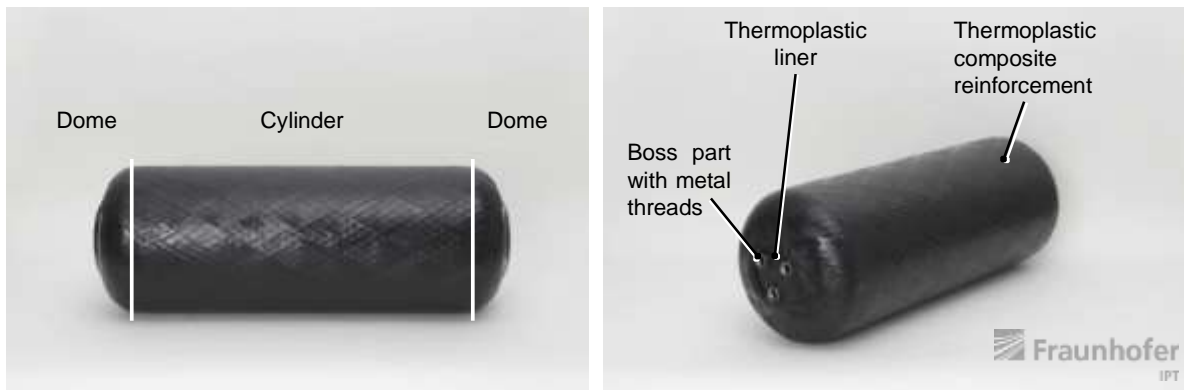


Figure 1. Type-IV thermoplastic composite pressure vessel

The typical production process for Type-IV pressure vessels consists of boss part manufacturing, liner formation e.g. by rotomolding or blow molding, liner annealing, thermoset composite application, multiple curing steps, hydro testing and gaseous leak testing and the assembly in the surrounding system [2]. For reinforcement, two types of winding patterns are used (see Figure 2): Hoop layers for reinforcement against tangential stresses and helical layers for reinforcement against mainly axial stresses [5].

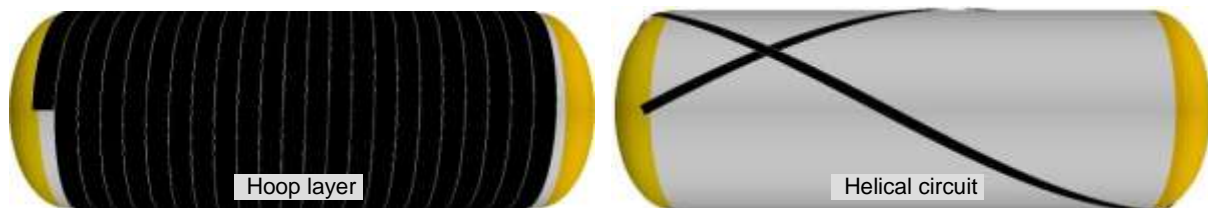


Figure 2. Visualization of hoop (left) and helical (right) winding patterns in CAD/CAM software

For the cost-effective production of CPVs, the reduction of the content of costly carbon fibers is key, which can be achieved by alternate liner geometries, alternate winding schemes and the use of alternate materials [2]. With respect to thermoset composites, which are mostly used for

pressure vessel reinforcement, thermoplastic composites feature advantages such as infinite storability, repeated formability, weldability, reparability, ease of handling and recycling capacity. They can be consolidated during layer application without subsequent curing steps – the so-called “in-situ consolidation” – which leads to lower manufacturing times [6,7].

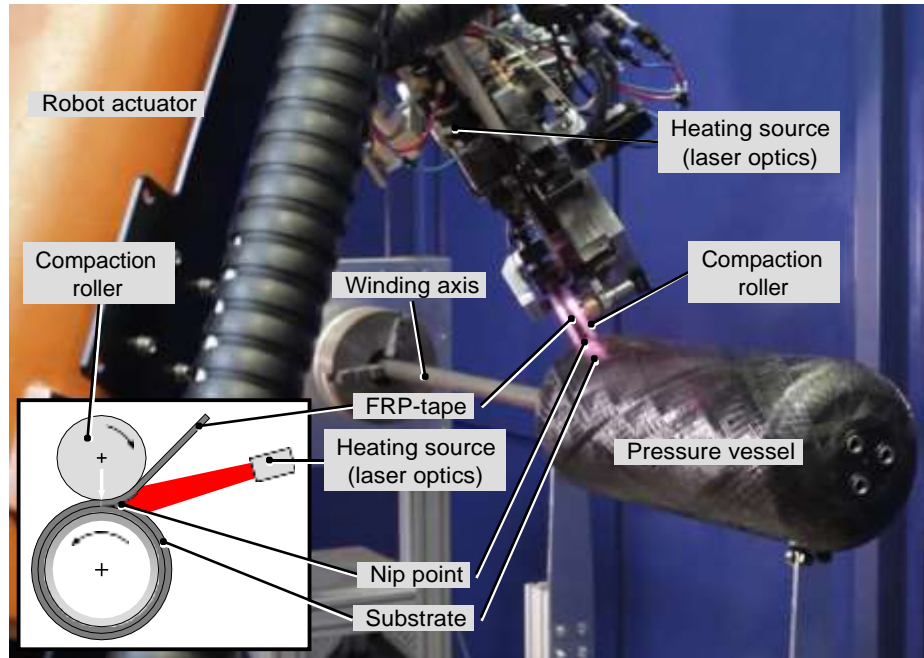


Figure 3. Laser-assisted tape winding – Process principle and application for CPV reinforcement (setup at Fraunhofer IPT)

One designated process for the reinforcement of thermoplastic pressure vessels is the application of tapes, pre-impregnated and pre-consolidated semi-finished materials, which are used in order to separate the impregnation process from the part manufacturing process and guarantee highest mechanical properties due to unidirectional fiber orientation [6,8]. Very few literature is available on the investigation of these products and their manufacturing. In [9], a thermoplastic CPV is manufactured by liner rotomolding and winding assisted by infrared heat. However, no investigation of the winding process was presented.

## 1.2 Laser-assisted tape winding

Laser-assisted tape winding (LATW) is a process suitable for the automated, fast and controlled manufacturing of thermoplastic composite parts [8]. The tape is wound around a liner or core while being simultaneously melted and consolidated by local application of heat and pressure in the nip point below the compaction roller (see Figure 3). While the pressure is applied by the compaction roller, the heating can be realized by open flame, hot air, hot gas, infrared heaters or laser irradiation [7]. The use of a diode laser enables fast and energy-efficient processing without preheating of the tape, fast and accurate temperature control, homogeneous intensity distributions, as well as low thermal effects on surrounding parts due to the localized heat input [8].

The most important parameters for process configuration are the irradiation intensity, tape feed rate and consolidation force. To achieve high, reproducible quality in the components

manufactured with in-situ consolidation, a high degree of process knowledge and process development is necessary [7]. This is especially relevant for the application of tapes on complex geometries like pressure vessels. In contrast to simple parts like pipes, the constantly varying substrate geometry and movements of the robot actuator induce varying tape feed rate and laser spot geometry. This causes non-stationary process conditions and thus temperature fluctuations affecting the consolidation quality of the produced part and posing the need for adapted processing strategies [10]. When these strategies are devised and implemented and tapes with low width are employed to minimize tape deformation, LATW is capable of application on complex geometries [11]. In this work, the varying process parameters for helical winding patterns are investigated to lay the groundwork for the development of advanced processing strategies.

## 2. EXPERIMENTATION

The main objective of the performed experiments was determining the effects of different process parameters on the temperature in the nip point during helical winding on a pressure vessel liner, as these encompass the dome regions and therefore induce non-stationary process conditions. As indicated above, the process temperature profile is indicative of the consolidation quality and thus the quality of the produced part [7,8,10].

### 2.1 System technology

For the implementation of the laser-assisted winding scheme, the tape placement applicator termed »Multi-Material-Head«, which was developed and assembled at Fraunhofer IPT, was used (see Figures 3 and 5). It was designed for the processing of multiple composite semi-finished materials – thermoplastic-based tapes, thermoset-based prepregs and dry-fiber materials – and consists of a material spool, guiding and feeding elements, a compaction unit for applying pressure, a laser-heating unit and a cutting unit [12]. The applicator is connected to a robot actuator providing the necessary degrees of freedom for helical winding, as the compaction roller always has to be positioned on the surface of the substrate to perpendicularly exert pressure into the nip point.

### 2.2 Materials and setup

Winding was performed on a pressure vessel liner out of PA6 (volume: 52 l, diameter: 304 mm, length: 770 mm). A glass fiber-reinforced PA6 tape from Celanese (width: 12 mm, thickness: 0.3 mm, fiber volume content: 60 %) was used. For these evaluative experiments, glass fiber reinforcement was used due to lower material cost. Further validations with carbon fiber-reinforced tape are planned. For path programming, the CAD/CAM software Compositcad was applied (see generated winding paths in Figure 2).

To eliminate first-layer effects from tape placement directly on the liner surface, which might arise due to different absorption and emission characteristics of liner and tape surfaces, a full helical layer was placed on the liner with process parameters determined in previous basic ramp-up trials. As displayed in Figure 4, additional layers were applied according to the experimental design of Table 1. The varied parameters were selected based on previous experiments evaluating the effect of parameter changes on the temperature in the nip point. Consolidation force was excluded from the experiments because it did not affect the temperature directly to a great extent. Inherent acceleration and jerk limits of the fixed robot actuator cause the tape feed rate to vary significantly from the set point, as evaluated in section 3.2. This is especially notable in the dome regions, where

measured speeds as low as 50 mm/s for a set point of 150 mm/s can occur. Because of this, the laser power is reduced in the dome regions in order to prevent overheating and thermal degradation of the composite. No closed-loop temperature control was applied to avoid temperature fluctuation effects described in [10].

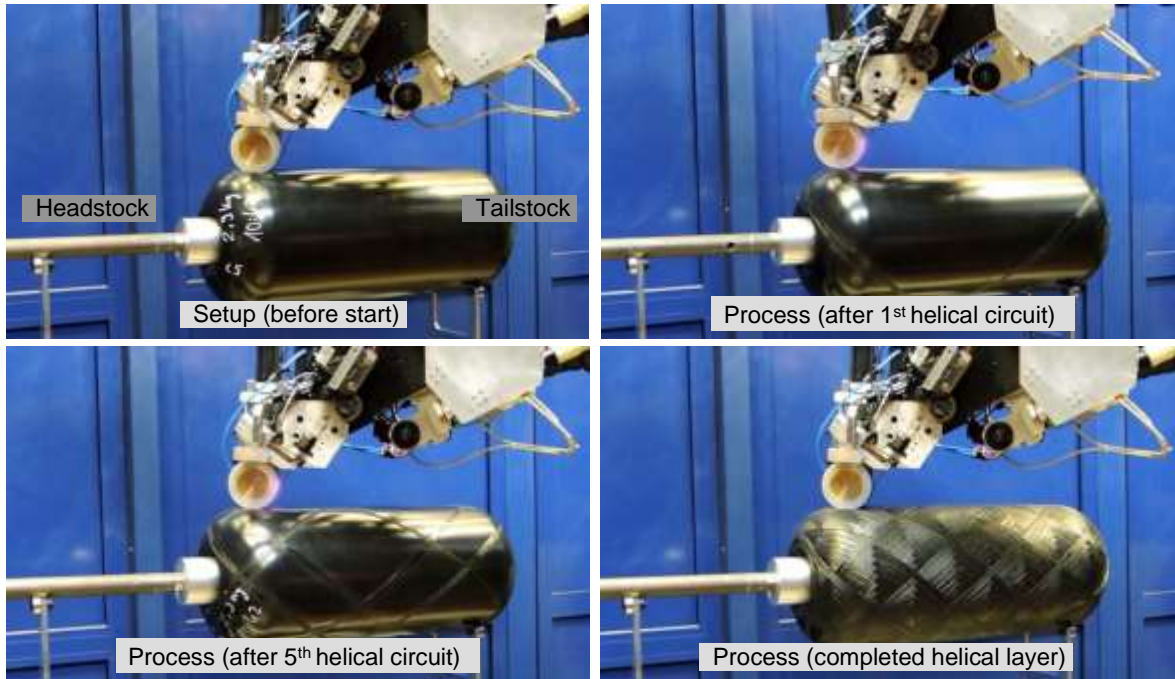


Figure 4. Experimentation setup and process

Table 1. Overview of experiments and parameter settings

Test code	Laser power [W]	Laser irradiation on tape [%]	Tape feed rate [mm/s]	Winding angle [°]
1.1	1200 W (cylinder), 600 W (domes)	55	150	38.7
2.1	1100 W (cylinder), 500 W (domes)	55	150	38.7
2.2	1300 W (cylinder), 700 W (domes)	55	150	38.7
3.1	1200 W (cylinder), 600 W (domes)	65	150	38.7
3.2	1200 W (cylinder), 600 W (domes)	45	150	38.7
4.1	1200 W (cylinder), 600 W (domes)	55	130	38.7
4.2	1200 W (cylinder), 600 W (domes)	55	170	38.7
5.1	1200 W (cylinder), 600 W (domes)	55	150	50
5.2	1200 W (cylinder), 600 W (domes)	55	150	30

### 2.3 Data acquisition and processing

During the experiments, the sensors integrated in the tape winding applicator (see Figure 5) were used to track process data including temperature, consolidation force exerted by the compaction roller, tape tension and tape feed rate. Temperature data was obtained with an infrared thermographic camera by DIAS Infrared (type: Pyroview 380 Lc) with a maximum frame rate of 50 Hz, a spectral range of 8-14  $\mu\text{m}$  and a resolution of 384 x 288 pixels. Temperature values for tape, nip point and substrate regions were extracted by defining regions of interest in the accompanying Pyrosoft software as depicted in Figure 5 and calculating mean temperatures for those regions. All experimental data was processed in the software MATLAB to determine the effects of parameter variation.

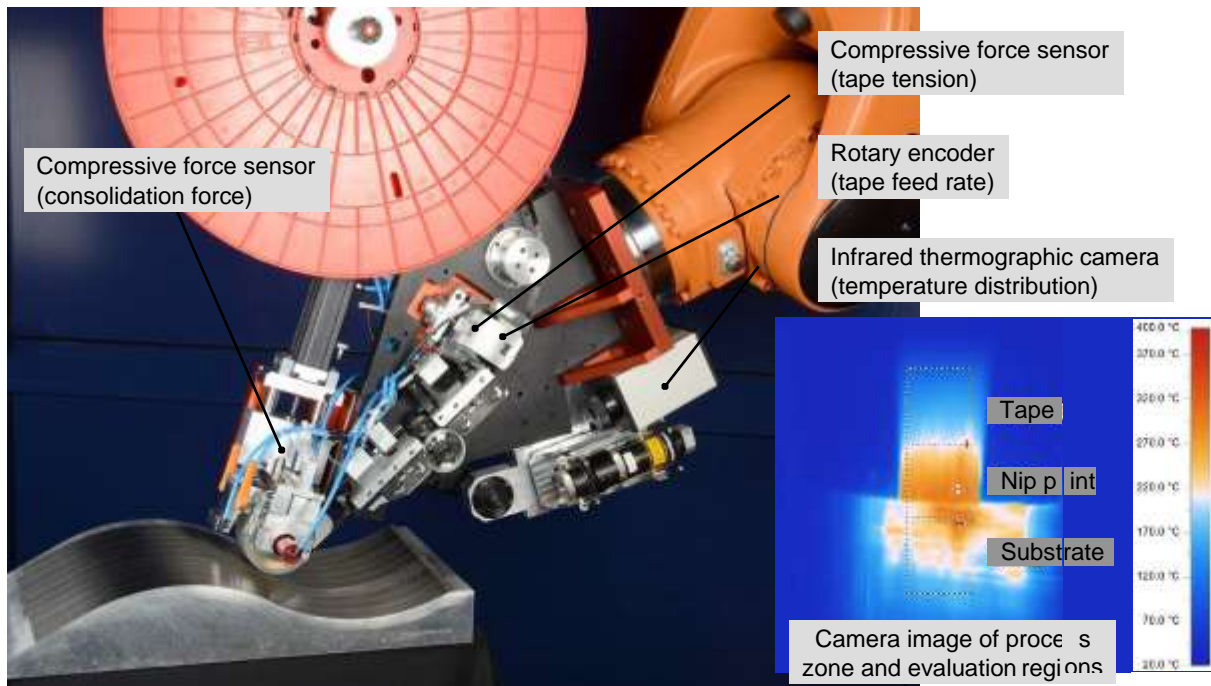


Figure 5. Sensor placement and temperature data processing in LATW system

## 3. RESULTS

In this section, the experimental results are evaluated. To reduce the amount of processable data, only the measurements of the first five helical circuits were processed and analyzed.

### 3.1 Assessment of process parameters

For a first assessment of the helical winding of thermoplastic CPV by LATW, the neutral case (see Table 1) was evaluated by calculating mean nip point temperatures for the cylinder and dome regions, differentiating between headstock and tailstock dome (see Figure 4). To prevent inclusion of transitional effects during the laser power changes, 10 % of the measured data at both beginning and end of each region was excluded. The results are displayed in Figure 6.

The temperatures in each region appear consistent over multiple helical circuits. For the cylindrical region, the mean nip point temperature is the same for the passage from headstock to tailstock as

vice versa. The nip point temperatures on the cylinder also lie well within the aspired process window above the melting temperature of PA6 (220 °C). On the contrary, the temperatures for both dome regions are mostly too low, indicating that the consolidation in these areas may not be achieved. In addition, the range between maximum and minimum nip point temperature on the dome regions, which is indicated by whisker plots in Figure 6, signifies high temperature fluctuations over the course of the dome regions, necessitating further assessment. Because of the observed similarities, further analysis will focus on three regions of interest: Cylinder, headstock dome and tailstock dome.

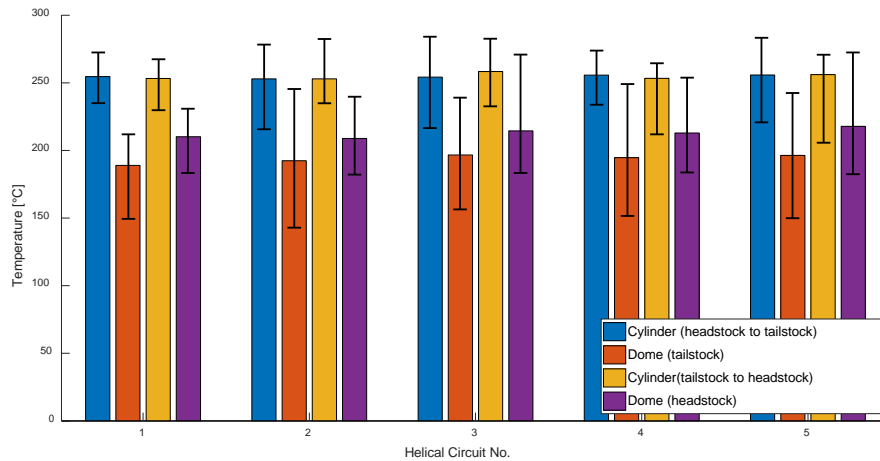


Figure 6. Mean nip point temperature of different regions for neutral case (test code 1.1; whisker plots indicate maximum and minimum nip point temperatures)

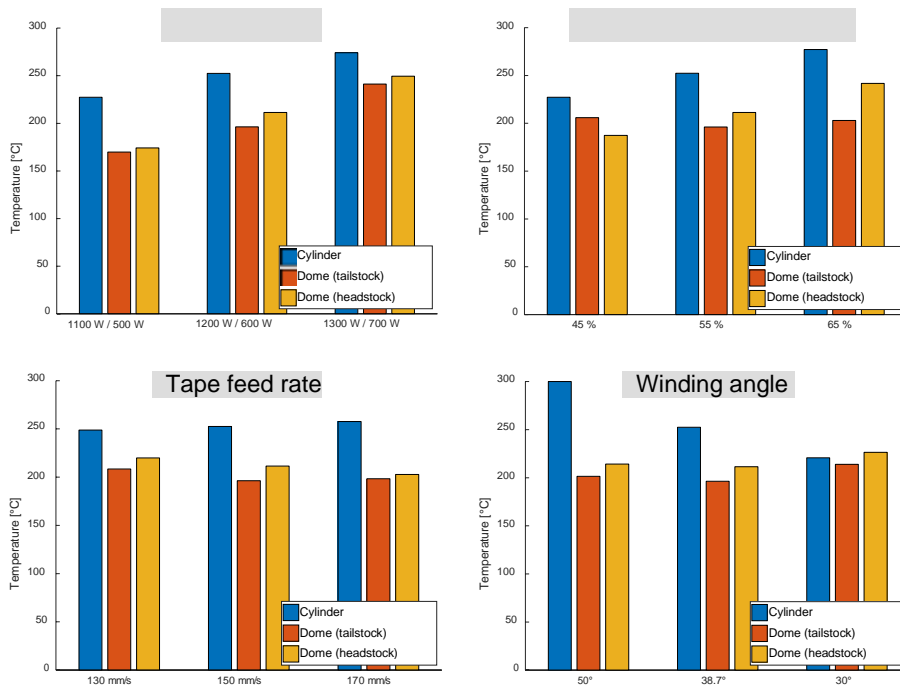


Figure 7. Comparison of mean nip point temperatures for variation of different process parameters

In Figure 7, the mean measured nip point temperature across the evaluated helical circuits for each of the parameter variation experiments is depicted for each critical region. The laser power experiments suggest a proportional relationship between laser power and temperature for all regions. For high levels of laser power, the disparity between cylinder and dome regions decreases slightly, indicating a more favorable heat input in the dome regions. Increasing the laser irradiation on tape correlates with increasing nip point temperatures for the cylinder and headstock dome. Surprisingly, the tailstock dome is not affected by the shift of the inclination angle of laser irradiation. Changing the tape feed rate seems to not have an influence on the temperature, which was not expected and led to further evaluation in section 3.2. Selecting a flat winding angle appears to have a strong negative relationship with the temperature in the cylindrical region and leading to an alignment between nip point temperatures between the cylinder and dome regions.

### 3.2 Evaluation of tape feed rate

On a first glance, the results of the parameter variation experiments for helical tape winding of CPV deviate significantly from expectations. Especially the considerable effect of winding angle change and the apparently absent effect of varied tape feed rate stand out. For this reason, a deeper investigation in the tape feed rate measurements during the experiments was conducted. Although the tape feed rate is explicitly given as a set point input into the CAD/CAM software, Figure 8 reveals that the actual tape feed rate diverges significantly from the set point. Apparent effects are the consistently reduced average speed in all regions, reoccurring instances of feed rate peaks and valleys in the dome regions, and high frequency fluctuations. A Butterworth 3<sup>rd</sup> order low pass filter with a cutoff frequency of 5 Hz was applied for to better evaluate the tape feed rate changes over time. As visualized in Figure 8, the filter introduces a small delay in response, especially during the transition between the regions where the feed rate changes significantly. However, the mean tape feed rates were not changed noticeably by this operation.

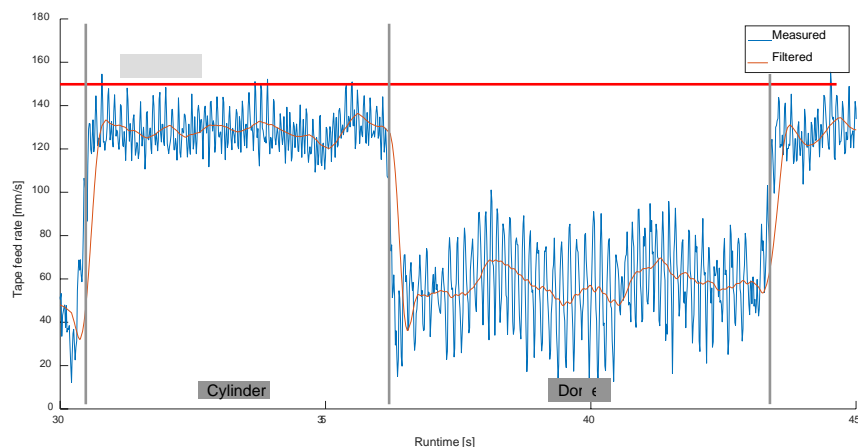


Figure 8. Tape feed rate before and after application of filter

The reduced average tape feed rate and the reoccurring deviations in the dome regions are thought to occur due to acceleration and jerk limits of the robot actuator when performing complex, multi-axes actuation of the tape winding applicator. To evaluate the effects of the varying tape feed rate on the nip point temperature, they are directly contrasted in Figure 9, taking into account the laser power, which was assumed to have the greatest effect on process temperature. In the figure, it can



be seen that the average nip point temperature varies accordingly to the set laser power for cylindrical and dome regions. However, within the regions there is a negative correlation between tape feed rate and temperature, contradicting the results displayed in Figure 7, which indicate no strong relationship between tape feed rate and temperature. For further analysis of this discrepancy, the tape feed rates for different regions were averaged for all performed experiments (see Figure 10). For the neutral case, variation of laser power and laser inclination angle, the average tape feed rates remain constant below the set point. For the variation of the tape feed rate set point, the measured tape feed rate in the cylindrical region remains nearly constant and there are only slight changes in the dome regions, amounting to a change of  $\pm 4$  mm/s for a set point adjustment of  $\pm 20$  mm/s. Adjustment of the winding angle has the greatest influence on the measured tape feed rate, especially in the cylindrical regions, where an angle decrease correlates with a feed rate increase.

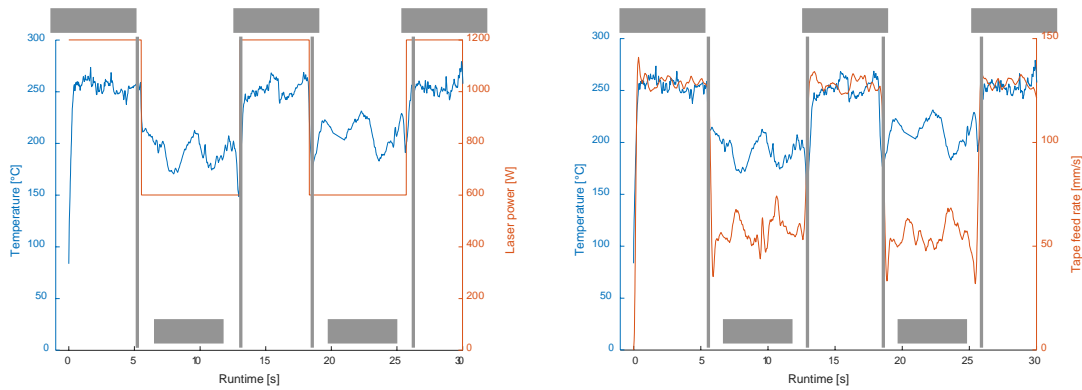


Figure 9. Effect of laser power (left) and tape feed rate (right) on nip point temperature for the neutral case (test code 1.1)

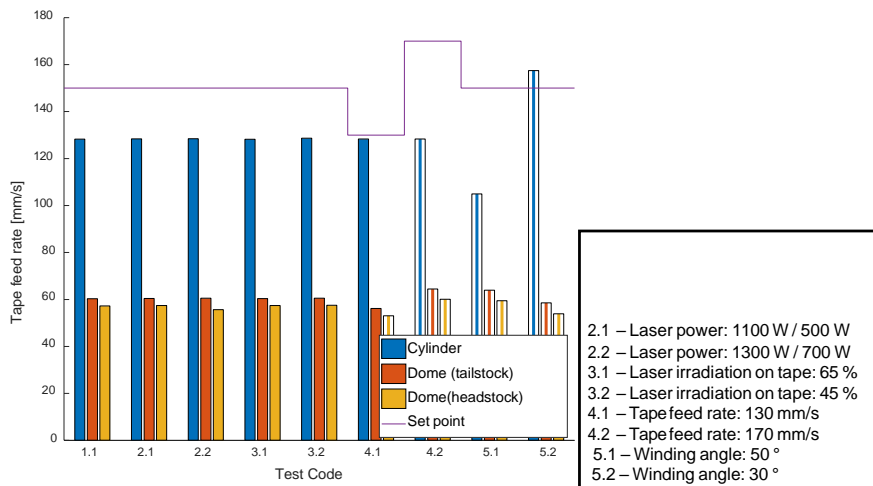


Figure 10. Comparison of mean tape feed rate for different experiments

The findings of this section indicate that the tape feed rate set in the CAD/CAM software and thus in the robot code has little effect on the actual measured tape feed rate. The changes of tape feed rate with changing winding angle explain the variations of nip point temperature in Figure 7. The

results displayed in Figure 10 also reveal that the tape feed rate at the headstock dome is consistently lower than that at the tailstock dome, corresponding to the consistently higher temperatures seen in the headstock dome regions in Figure 7. This is most probably due to the robot actuator having to extend very far from its base position, which requires more complex and precise actuation to maintain accurate inverse kinematics.

### 3.3 Development of empirical model

For further exploration of the effect of parameter variation on experimental validation data, an empirical model was derived from the experimental results. The parameter relationships suggested by assessments of sections 3.1 and 3.2 are summarized in Table 2.

Table 2. Relationships between evaluated parameters and nip point temperature

Parameter [unit]	Suggested relationship to nip point temperature $T_{nip}$ [unit: °C]
Tape feed rate $v_{Tape}$ [mm/s]	$\Delta T_{nipp} \propto \frac{1}{v_{Tape}}$
Laser power $P_{Laser}$ [W]	$\Delta T_{nipp} \propto P_{Laser}$
Laser inclination angle $\varphi$ [°]	$\Delta T_{nipp} \propto \varphi$
Winding angle [°]	No relationship

Modelling the relationship between tape feed rate and nip point temperature was considered first, due to the constant variation of the feed rate from the set point pointed out in the previous section (see Figure 10). According to the relationship expressed in Table 2, the proportionality factor  $a$  is introduced and an ambient temperature  $T_{ambient}$  was considered, leading to equation [1].

$$T_{nipp} = a \cdot \frac{1}{v_{Tape}} + T_{ambient} \quad [1]$$

In this case,  $a$  is a function of all LATW process parameters except  $v_{Tape}$ . The proportionality factor was determined according to equation [1] using the determined mean tape feed rates and nip point temperatures for the neutral case (test code 1.1 in Table 1) and differentiating between cylinder, headstock dome and tailstock dome. As visualized in Figure 11, good agreement between this simplistic model and the measured data is obtained both in absolute temperature values and in temperature changes due to tape feed rate variation. Since the tape feed rate is the only variable parameter when considering temperature fluctuations in the different CPV regions, Figure 11 confirms the relationship between measured nip point temperature and tape feed rate.

Based on these results, the empirical model was extended to include the relationships of temperature with laser power and laser inclination angle affecting the laser irradiation shares of tape and substrate. In equation [2],  $b$  is the proportionality factor expressing the relationship of nip point temperature with laser power and tape feed rate for a fixed reference laser inclination angle. Similarly,  $c$  is the proportionality factor for a change of laser inclination angle with respect to the reference angle. Both proportionality factors were determined by linear regression, with the

determination of  $b$  taking into account experiments 2.1 and 2.2 and the determination of  $c$  taking into account experiments 3.1 and 3.2, respectively, in addition to the neutral case. In Figure 12, the measured and modeled temperature values are contrasted for experiment 4.1.

$$T_{\text{nip}} = \frac{PP_{LLTLLTLL}}{VV_{TTTTnrTT}} + cc \cdot \phi\phi - \phi\phi_{TT} + T_{TaaaanTnnn} \quad [2]$$

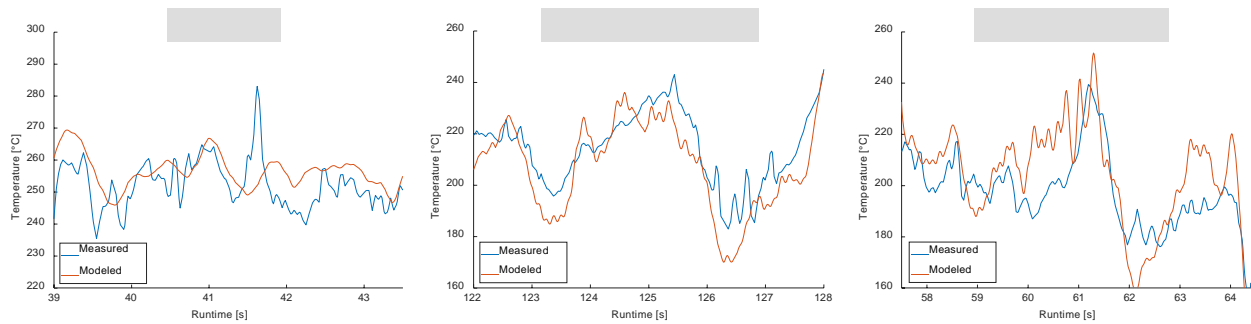


Figure 11. Comparison of modeled and measured nip point temperature based on tape feed rate in different regions (neutral case, test code 1.1)

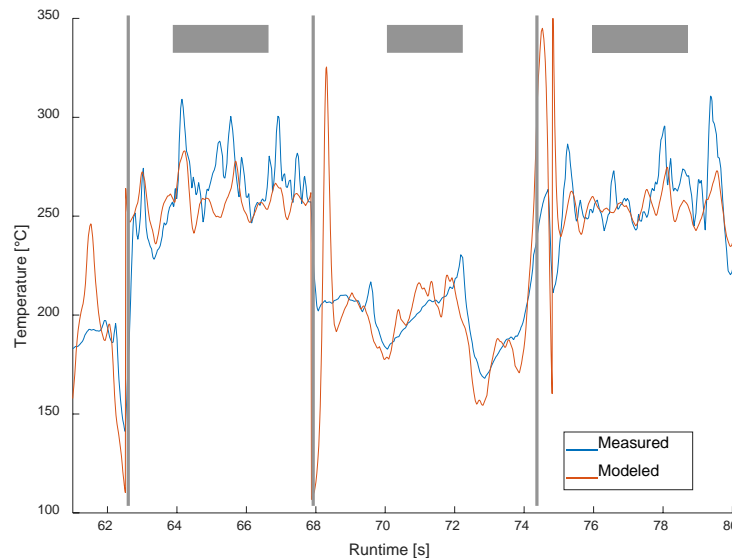


Figure 12. Comparison of measured and modeled nip point temperature (test code 4.1)

In general, the response of the empirical model agrees well with the measured data. The large spikes in the modelled response are due to instantaneous changes in laser power combined with the delay associated with acceleration and deceleration of the tape feed rate. Since the model does not consider any transient heat transfer effects, this causes inaccurate temperature predictions in these transition regions. Overall, the model confirms the relationships of the nip point temperature with the evaluated process parameters and can be applied for parameter adjustment in future process optimization efforts. Due to the simplicity of the model, it can be used for quick online modelling and adjustment of process parameters.

### 3.4 Assessment of winding around dome parts

First evidenced in Figure 6 and further proven in the previous sections, the dome sections pose a significant challenge for process design due to high fluctuations of tape feed rate and varying irradiated substrate area, which has an effect on the selection of the laser inclination angle and thus the irradiation shares on tape and substrate (see also [10]). Adjusted strategies are necessary for either levelling of tape feed rate fluctuations or adjustment of laser power and laser inclination angle with the goal of maintaining a constant nip point temperature above the melting temperature of the polymer.

Differences between headstock and tailstock dome regions were observed due to deviating tape feed rates affected by the extended position of the robot actuator. In addition, changes of the laser irradiation share on the tape seem to have different effects for the two dome regions, as evidenced in Figure 7. This was confirmed in the development of the empirical model, where the proportionality factors  $a$  and  $b$  were similar for both dome regions, while the third proportionality factor  $c$  associated with the laser inclination angle varied considerably for both regions. Further analysis was conducted on the images of the infrared thermographic camera, which led to the assumption that these effects can also be traced to the robot actuator movements, leading to a less smooth path and varying compaction roller deflections when the robot is extended.

Collectively, these observations lead to the assessment that the manufacturing environment has to be taken into account when devising processing strategies for LATW of complex geometries. The position, size and acceleration and jerk limits of the robot highly affect the tape feed rates and consequently the nip point temperature. Different winding angles leading to different robot positions influence these parameters, as displayed in Figure 13 by contrasting the tested winding angles with measured tape feed rate and nip point temperature measured within the process as well as determined by the empirical model.

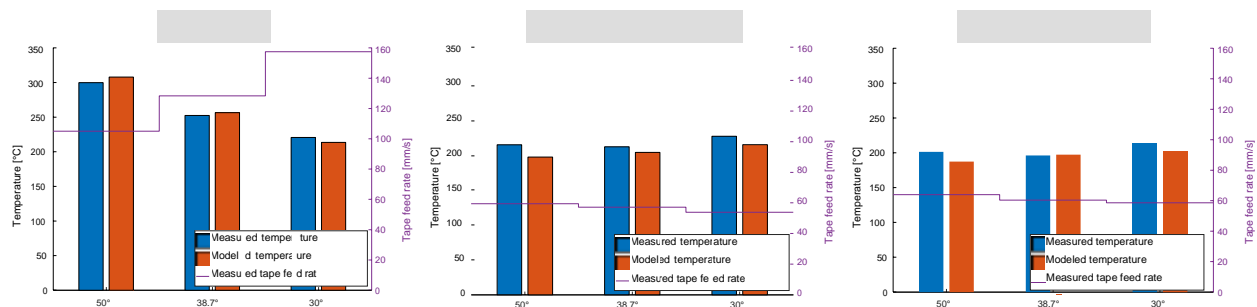


Figure 13. Comparison of measured and modeled nip point temperature including measured tape feed rate for different regions and winding angles

## 4. CONCLUSIONS

A sequence of process parameter investigation experiments was performed for the manufacturing of reinforcement layers of a Type-IV thermoplastic composite pressure vessel by laser-assisted tape winding. The results show dependencies of the measured nip point temperature on laser power, tape feed rate and laser irradiation shares of tape and substrate. The tape feed rate diverges significantly from the point set in the CAD/CAM software and is influenced by varying robot speeds for different set winding angles. An empirical model was derived confirming the observed

- 13 Postprint. Erstveröffentlichung: Schäkel, Martin; Janssen, Henning; Brecher, Christian (2021): Process Analysis of Manufacturing Thermoplastic Type-IV Composite Pressure Vessels with Helical Winding Pattern. International SAMPE Conference and Exhibition (SAMPE 2021); Volume 2 of 2. S. 877-889. Red Hook, NY: Curran.

relationships and pointing towards the need for adjusted processing strategies for obtaining consistent consolidation quality in the dome regions. An increased effort in process modelling will be pursued to achieve indications for adjustments of laser power and laser inclination angle within the process. In integrative approach including CAD/CAM programming and process design under consideration of the manufacturing infrastructure is necessary for achieving reproducible and reliable quality of these highly safety-relevant components and to allow for an increased pick-up of thermoplastic composite parts in industrial applications.

## 5. REFERENCES

- [1] Sachgau, O. & Behrmann, E. "The Hydrogen-Powered Car's Big Setback." *Bloomberg*. March 23, 2018. <<https://www.bloomberg.com/news/articles/2018-03-23/the-hydrogen-powered-car-s-big-setback>>
- [2] James, B.D., Houchins, C., Huya-Kouadio, J.M. & DeSantis, D.A. "Final Report: Hydrogen Storage System Cost Analysis." United States Department of Energy. September, 2016. DOI: 10.2172/1343975.
- [3] Red, Chris. "Pressure vessels for alternative fuels, 2014-2023." *Composites World*. January 12, 2014. <<https://www.compositesworld.com/articles/pressure-vessels-for-alternative-fuels-2014-2023>>
- [4] Holmes, Mark. "High volume composites for the automotive challenge." *Reinforced Plastics* 61(5) (2017): 294-298. DOI: 10.1016/j.repl.2017.03.005.
- [5] Romagna, Jürg Herbert. "Neue Strategien in der Faserwickeltechnik." Dissertation ETH Zürich, 2017. DOI: 10.3929/ethz-a-001945867.
- [6] Mallick, P.K. "Fiber-reinforced Composites." Boca Raton, United States: CRC Press, 2007.
- [7] Mazumdar, Sanjay K. "Composites Manufacturing – Materials, Product and Process Engineering," Boca Raton, United States: CRC Press, 2000.
- [8] Steyer, Martin. "Laserunterstütztes Tapelegeverfahren zur Fertigung endlosfaserverstärkter Thermoplastlaminat." Dissertation RWTH Aachen, 2013.
- [9] Villalonga, A., Thomas, C., Nony, F., Thiebaud, F., Geli, M., Lucas, A., Kremer-Knobloch, K. & Maugy, C. "Application of full thermoplastic composite for Type IV 70 MPa high pressure vessels." *Proceedings of 18<sup>th</sup> International Conference on Composite Materials*. Jeju Island, South Korea, August 21-26, 2011. The Korean Society of Composite Materials.
- [10] Kollmannsberger, Andreas M. "Heating characteristics of fixed focus laser assisted Thermoplastic-Automated Fiber Placement of 2D and 3D parts." Dissertation TU München, 2019.
- [11] Kermer-Meyer, Alexander. "Formhaltige and komplexe Laminatstrukturen in Thermoplast-Tapelegeverfahren." Dissertation RWTH Aachen, 2015.
- [12] Brecher, C., Werner, D. & Emonts, M. "Multi-Material-Head – One tool for 3 technologies: Laser-assisted thermoplast-tape placement, thermoset-prepreg-placement and dry-fiber placement." *Proceedings of the 20<sup>th</sup> International Conference on Composite Materials*. Copenhagen, Denmark, July 19-24, 2015. MCI Copenhagen.